CrossMark
click for updates

View Article Online
View Journal

RSC Advances

This article can be cited before page numbers have been issued, to do this please use: L. Cartwright, L. J. Taylor, H. Yi, A. Iraqi, Y. Zhang, N. Scarratt, T. Wang and D. G. Lidzey, *RSC Adv.*, 2015, DOI: 10.1039/C5RA20927G.

This is an *Accepted Manuscript*, which has been through the Royal Society of Chemistry peer review process and has been accepted for publication.

Accepted Manuscripts are published online shortly after acceptance, before technical editing, formatting and proof reading. Using this free service, authors can make their results available to the community, in citable form, before we publish the edited article. This *Accepted Manuscript* will be replaced by the edited, formatted and paginated article as soon as this is available.

You can find more information about *Accepted Manuscripts* in the Information for Authors.

Please note that technical editing may introduce minor changes to the text and/or graphics, which may alter content. The journal's standard Terms & Conditions and the Ethical guidelines still apply. In no event shall the Royal Society of Chemistry be held responsible for any errors or omissions in this *Accepted Manuscript* or any consequences arising from the use of any information it contains.

ROYAL SOCIETY OF CHEMISTRY

www.rsc.org/advances

Please do not adjust margins
View Article Online
DOI: 10.1039/C5RA20927G

Journal Name

ARTICLE

Published on 18 November 2015. Downloaded by UNIVERSITY OF OTAGO on 20/11/2015 05:59:15.

Triisopropylsilylacetylene-Functionalised Anthracene-*alt*-Benzothiadiazole Copolymers for Application in Bulk Heterojunction Solar Cells

Received 00th January 20xx,
Accepted 00th January 20xx

DOI: 10.1039/x0xx00000x

www.rsc.org/

Luke Cartwright,[a] Lois. J. Taylor,[a] Hunan Yi,[a] Ahmed Iraqi,*[a] Yiwei Zhang,[b] Nicholas. W. Scarratt,[b] Tao Wang,[c] and David. G. Lidzey*[b]

Three triisopropylsilylacetylene-functionalised anthracene (TIPSAnt) based polymers were synthesised by copolymerising TIPSAnt with either dithienyl-5,6-difluoro-benzo[*c*]-[1,2,5]thiadiazole, dithienyl-benzo[*c*]-[1,2,5]thiadiazole or dibithiophenyl-benzo[*c*]-[1,2,5]thiadiazole to yield **PTATffBT**, **PTATBT-8** and **PTAT2BT-8**, respectively. **PTAT2BT-8** demonstrated a reduced optical and electrochemical band gap, relative to **PTATffBT** and **PTATBT-8**. The HOMO level of **PTAT2BT-8** (-5.32 eV) is significantly shallower compared to its counterparts. This can be attributed to increased intramolecular charge transfer along the polymer backbone; a consequence of the incorporation of additional thiophene spacer units. The photovoltaic properties of the polymers were investigated by fabricating bulk heterojunction (BHJ) polymer solar cells using $PC_{70}BM$ as the electron acceptor. **PTATffBT** displayed limited solubility in common organic solvents and could not be used for the fabrication of photovoltaic cells. Optimised photovoltaic devices fabricated from **PTATBT-8** and **PTAT2BT-8** demonstrated power conversion efficiencies of 2.36 % and 3.15 %, respectively. **PTAT2BT-8** provided better efficiencies chiefly as a result of better J_{sc} and *FF* values.

Introduction

The combustion of fossil fuels releases carbon dioxide; a gas that accentuates the greenhouse effect and climate change. This has prompted the scientific community to develop new forms of renewable energy. Polymer solar cells (PSC) have the potential to provide a clean source of energy owing to their ease of fabrication and low production costs.[1,2]

The most successful PSCs to date are devices fabricated using a bulk heterojunction (BHJ) active layer architecture.[3–6] An n-type material, commonly a fullerene derivative, is blended with a conjugated polymer, p-type material to form a nanoscale, bicontinous interpenetrating network.[7] Fullerene derivatives find wide-scale application as near ideal n-type materials for PSCs.[8–10] However, the development of new donor-acceptor (D-A) alternating conjugated copolymers is essential if the efficiencies of PSCs are to rival inorganic devices.[11] It is important that the conjugated polymer has a low optical band gap, high absorption coefficients, finely tuned frontier energy levels and high hole mobilities.[12] Such conjugated polymers must ideally have excellent solubility in common organic solvents to ensure the photovoltaic device can be fabricated using low-cost solution based processing.[13,14] Kallmann and Pope were the first to investigate the photovoltaic effect in organic anthracene crystals.[15] Since then, the body of work covering anthracene and its optoelectronic properties has been extended. Anthracene and the acene family in general, possess extended π-conjugated systems resulting in planar molecules with a high degree of crystallinity.[16] π-conjugated systems aid electron transfer along the polymer backbone resulting in high charge mobility. Furthermore, anthracene is an extremely versatile molecule and can be polymerised through its 2,6-positions or 9,10-positions.[17–22] Providing that the polymerisation is conducted through the 2,6-positions, the 9,10-positions can be functionalised with substituents; affording a way to tune the optoelectronic properties of the resulting polymer.[19] Consequently, anthracene and its derivatives have found widespread use in organic-field effect transistors and organic light emitting diodes.[23–27]

The use of anthracene in PSC is limited, which is surprising considering that benzo[1,2-*b*:4,5-*b*']dithiophene (BDT), which has an analogous molecular framework, has found widespread use in high performance PSC devices.[28–32] Park *et al* reported a new class of anthracene-thiophene based copolymers incorporating bulky triisopropylsilylacetylene (TIPS) groups at the 9,10-positions of the anthracene moiety.[32] It was reported that the incorporation of TIPS groups overcame the poor

[a] Department of Chemistry, University of Sheffield, Sheffield, S3 7HF, UK. E-mail: a.iraqi@sheffield.ac.uk; Fax: +44 (0)114 222 9303; Tel: +44 (0)114 222 9566
[b] Department of Physics and Astronomy, University of Sheffield, S3 7RH, UK.E-mail d.g.lidzey@sheffield.ac.uk; Fax: +44 (0)114 222 3555; Tel: +44 (0)114 222 3501
[c] School of Materials Science and Engineering, Wuhan University of Technology, Wuhan 430070, China.

Electronic Supplementary Information (ESI) available: ^{1}H, ^{13}C of **M1**. ^{1}H NMR spectra of the polymers. See DOI: 10.1039/x0xx00000x

RSC Advances Accepted Manuscript

View Article Online
DOI: 10.1039/C5RA20927G

Published on 18 November 2015. Downloaded by UNIVERSITY OF OTAGO on 20/11/2015 05:59:15.

charge transportation properties and high crystallinity that are generally associated with polythiophene-based copolymers. The polymer yielded efficiencies of 1.70 % when blended with $PC_{60}BM$ and used as the active layer in a BHJ photovoltaic device.[32] Iraqi and co-workers presented the preparation of donor-acceptor polymers with alternating 2,6-linked anthracene units with aryloxy substituents at their 9,10-positions and various benzothiadiazole alternate repeat units. Efficiencies ranging from 1.93 to 4.17 % were measured for these polymers.[33] More recently, Jo and co-workers synthesised a copolymer composed of thienyl substituted anthracene and diketopyrrolopyrrole. The resulting polymer exhibited an efficiency of 7.02 % and 4.23 % when blended with $PC_{70}BM$ and di-perylene bisimide, respectively.[18]

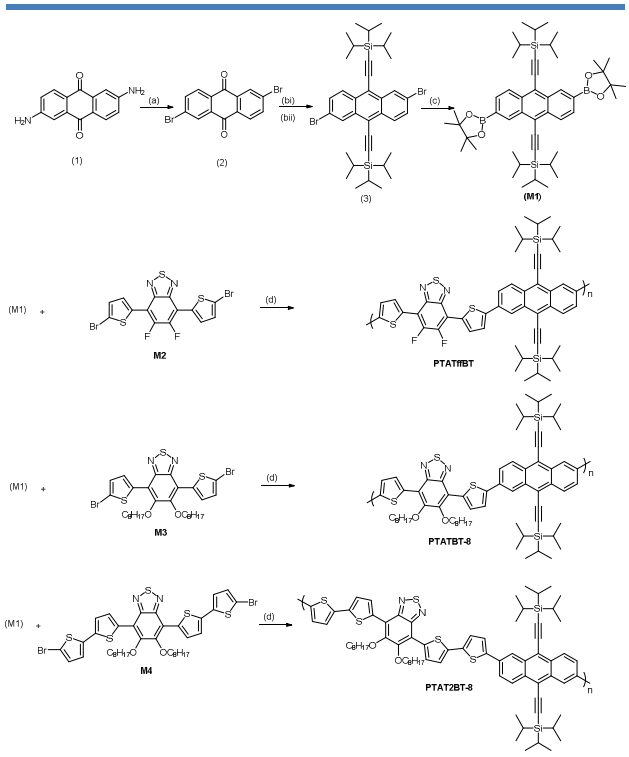

Scheme 1. Synthesis of 2,6-bis-4,4,5,5-tetramethyl-1,3,2-dioxaborolan-2-yl)-9,10-bis(triisopropylsilylacetylene) anthracene (4): (a) $CuBr_2$, *t*-BuONO, CH_3CN; (b*i*) *n*-BuLi, TIPS, THF, 24 hours; (b*ii*) $SnCl_2$, HCl (10 % aq); (c) bis(pinacolato)diboron, KOAc, Pd(dppf)Cl_2, DMF; (d) $Pd(OAc)_2$, P(*o*-tolyl)$_3$, NEt_4OH, toluene.

Here, we report the synthesis and optoelectronic properties of three anthracene-*alt*-benzothiadiazole donor-acceptor copolymers, **PTATffBT**, **PTATBT-8** and **PTAT2BT-8**. The study focusses on incorporating TIPS groups at the 9,10-positions of the anthracene unit and the impact of various benzothiadiazole acceptors. **PTATffBT** was highly insoluble and photovoltaic devices could not be fabricated from this polymer. Organic photovoltaic devices based on **PTATBT-8** and **PTAT2BT-8** display power conversion efficiencies (PCEs) of 2.36 % and 3.15 %, respectively, when blended with $PC_{70}BM$ in BHJ photovoltaic devices.

Results and Discussion

Monomer and Polymer Synthesis

The preparation of monomers and polymers are outlined in Scheme 1. Anthracene dibromide (**3**) was prepared according to literature procedures.[34] It was then converted to the bis-boronate ester (**M1**) upon reaction with bis(pinacolato)diboron in the presence of Pd(dppf)Cl_2.

M4 was then reacted with **M2**, **M3** and **M4**, *via* Suzuki coupling, in the presence of $Pd(OAc)_2$ and tri(*o*-tolyl)phosphine, to yield **PTATffBT**, **PTATBT-8** and **PTAT2BT-8**, respectively. The polymers were fractionated *via* Soxhlet extraction using the solvents; methanol, acetone, hexane and toluene. All polymers were obtained as deep purple powders. The yield of **PTAT2BT-8** was significantly lower than **PTATffBT** and **PTATBT-8** and large amounts of insoluble polymer remained in the thimble after Soxhlet extraction. This suggests that the incorporation of additional thiophene units together with the small solubilising TIPSsubstituents positioned on the anthracene unit were not able to facilitate the processability of the high molecular mass fraction of the polymer. Despite large quantities of **PTATffBT** being extracted in the toluene fraction, it should be noted that **PTATffBT** exhibited poor solubility in common organic solvents such as chloroform, chlorobenzene, *o*-dichlorobenzene and 1,2,4-trichlorobenzene at elevated temperatures. Consequently, photovoltaic devices could not be fabricated from **PTATffBT**. The chemical structures of **PTATffBT**, **PTATBT-8** and **PTAT2BT-8** were confirmed *via* ^{1}H-NMR and elemental analysis. The number average molecular weight (M_n) and weight average molecular weight (M_w) of all polymers were measured using high-temperature (140^{o}C) gel permeation chromatography (GPC) using 1,2,4-trichlorobenzene as the eluent and polystyrene as the internal standard (Table 1). **PTATBT-8** displayed a M_n of 13,600 and a M_w of 38,700 Da. **PTAT2BT-8** displayed a reduced M_n (6,600 Da) and a M_w (13,200 Da) relative to PTATBT-8, which can be attributed to the incorporation of additional thiophene-spacer units without solubilising groups. **PTATffBT** displayed significantlyreduced M_n and M_w values of 2,100 Da and 2,500 Da, respectively as a result of the absence of solubilising substituents on the **TffBT** units. Furthermore, previous studies have also indicated that incorporation of fluorine on the benzothiadiazole-moiety facilitates stronger π-π stacking and aggregation of polymer chains, which severely limits accessibility to high molecular weight materials.[35,36]

Optical Properties

The absorption spectra of the polymers were recorded both in solution (chloroform) and as drop-cast films (Figure 1). The

RSC Advances Accepted Manuscript

This journal is © The Royal Society of Chemistry 20xx

Please do not adjust margins
View Article Online
DOI: 10.1039/C5RA20927G

Journal Name

ARTICLE

Published on 18 November 2015. Downloaded by UNIVERSITY OF OTAGO on 20/11/2015 05:59:15.

Table 1.GPC data, UV-Vis data, energy levels and energy gaps of the polymers

Polymer	M_n (Da)[a]	M_w (Da)[a]	λ_{max} Solution (nm)	λ_{max} Film (nm)	E_{gopt} (eV)[b]	HOMO (eV)[c]	LUMO (eV)[d]	E_{gelec} (eV)[e]
PTATffBT	2,100	2,500	357, 455, 520	328, 469, 523	1.92	-5.48	-3.16	2.32
PTATBT-8	13,600	38,700	344, 524	369, 555	1.85	-5.46	-3.42	2.04
PTAT2BT-8	6,600	13,200	395, 540	402, 566	1.81	-5.31	-3.47	1.84

[a]Measurements conducted on the toluene fractions of polymers using a differential refractive index (DRI) detection method. [b]Optical energy gap determined from the onset of the absorption band in thin film.[c]HOMO position (*vs* vacuum) determined from the onset of oxidation. [d]LUMO position (*vs* vacuum) determined from the onset of reduction. [e]Electrochemical energy gap.

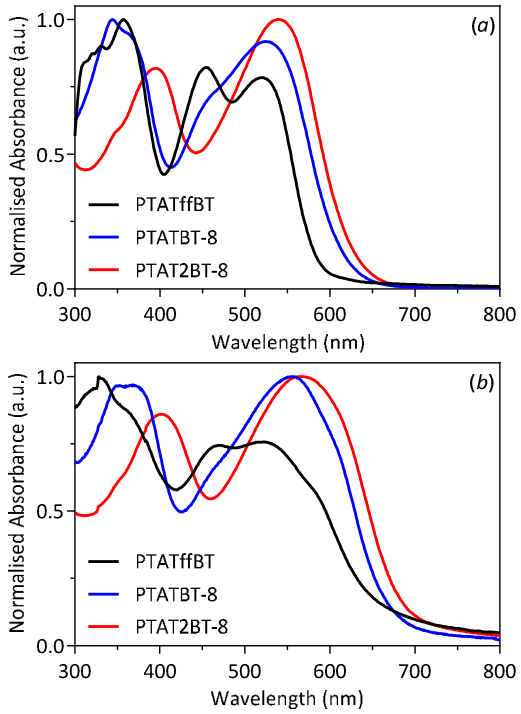

Figure 1. Normalised absorption spectra of **PTATffBT**, **PTATBT-8** and **PTAT2BT-8** in: (*a*) chloroform solutions; and (*b*) thin films.

optical band gap and absorption value maxima are shown in Table 1. PTATffBT displays absorptions maxima at 357, 455 and 520 nm in chloroform solution and at 328, 469 and 523 nm in films. The lack of a significant bathochromic shift from solution to film indicates that the polymers adopt similar energetic conformations in both solution and film states. The additional peaks in the UV-vis spectra of **PTATffBT** are attributed to the inhomogeneously-broadened electronic and vibrational transitions of the polymer. The optical band gap of **PTATffBT** was calculated to be 1.92 eV. The large optical band gap can be attributed to the low molecular weight of **PTATffBT**.

PTATBT-8 displays absorption bands in the visible region at 524 and 556 nm, in chloroform solution and film states, respectively. The bathochromic shift that is observed from solution to film can be ascribed to a more coplanar structure in solid state. **PTAT2BT-8** displays a maximum at 540 nm in chloroform solution. The absorption maximum of **PTAT2BT-8** is red-shifted to 566 nm when cast into a thin-film. The intramolecular charge transfer (ICT) band in the solid-state optical spectrum of **PTAT2BT-8** is more pronounced relative to the π-π* band. This phenomenon is not evident in **PTATBT-8**. Furthermore, the optical band gap of **PTAT2BT-8** (1.81 eV) is lower than that of **PTATBT-8** (1.85 eV). We speculate that the incorporation of a bithiophene spacer-unit facilitates intramolecular charge transfer along the polymer backbone resulting in increased electronic delocalisation and a reduced optical band gap. The optical band gaps of **PTATBT-8** and **PTAT2BT-8** are located close to the maximum solar flux.

PTATBT-8 and **PTAT2BT-8** are analogous to two polymers previously synthesised by Iraqi and co-workers (**PPATBT-8** and **PPAT2BT-8**).[33] In **PPATBT-8** and **PPAT2BT-8** the anthracene moiety is functionalised with 4-dodecyloxybenzene groups, instead of TIPS. **PPATBT-8** and **PPAT2BT-8** have optical band gaps of 1.96 and 1.86 eV, respectively.[33] We speculate that the acetylene group and the long C-Si bond present in TIPS locate the solubilising alkyl chains further away from the conjugated backbone, which facilitates planarization of the polymer backbone and improves π-π interchain stacking. This result is consistent with the reduced M_n and M_w values obtained for **PTATBT-8** and **PTAT2BT-8**, relative to **PPATBT-8** and **PPAT2BT-8**.

RSC Advances Accepted Manuscript

Please do not adjust margins

View Article Online
DOI: 10.1039/C5RA20927G

Published on 18 November 2015. Downloaded by UNIVERSITY OF OTAGO on 20/11/2015 05:59:15.

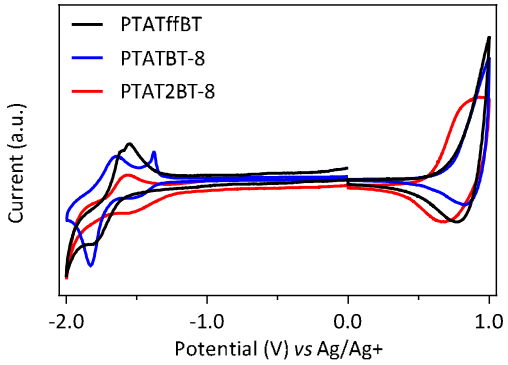

Figure 2. Cyclic voltammograms of **PTATffBT**, **PTATBT-8** and **PTAT2BT-8** on platinum disc electrodes (area 0.031 cm^2) recorded at a scan rate of 100 mV s^{-1} in acetonitrile/tetrabutylammonium perchlorate (0.1 mol dm^{-3}).

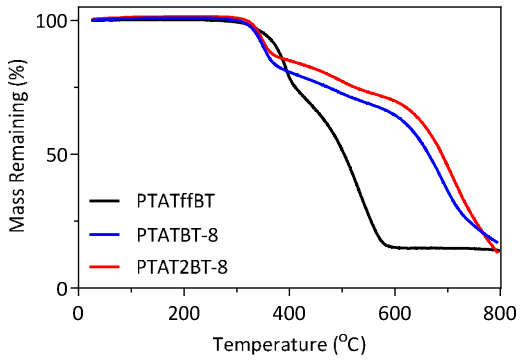

Figure 3. TGA plots of **PTATffBT**, **PTATBT-8** and **PTAT2BT-8**with a heating rate of 10 °C min^{-1} under an inert atmosphere of nitrogen.

Electrochemical Properties

The frontier energy levels (*vs* vacuum) of the polymers were determined from the onsets of oxidation and reduction (Table 1). The onsets were determined *via* cyclic voltammetry measurements, which were conducted on drop-cast polymer films in acetonitrile with tetrabutylammonium perchlorate as the electrolyte (Figure 2). The HOMO/LUMO levels of **PTATffBT**, **PTATBT-8** and **PTAT2BT-8** were estimated to be -5.48/-3.16 eV, -5.46/-3.42 eV and -5.31/-3.47 eV, respectively. The shallower HOMO level of **PTAT2BT-8** relative to that of **PTATBT-8** occurs as a result of increased intramolecular charge transfer along the polymer backbone. Such effects are a consequence of incorporating bithiophene spacer-units into the polymer backbone. However, the LUMO level of **PTAT2BT-8** is at a similar energy level to that of **PTATBT-8**.

PTATffBT has the deepest HOMO level of all polymers synthesised within this report; a consequence of substituting octyloxy groups on the benzothiadiazole-moiety for fluorine. This result is consistent with previous literature that shows that fluorination of acceptor moieties yields deeper HOMO levels.[35–38] However, the LUMO level of **PTATffBT** is significantly shallower relative to both **PTATBT-8** and **PTAT2BT-8**. This is not consistent with previous literature findings. We speculate that the low molecular weight of **PTATffBT** is responsible for this observation. Previous literature has shown that the LUMO level of a polymer decrease more rapidly relative to the HOMO level as the molecular weight increases.[39] This is attributed to molecular orbital hybridisation of each monomer resulting in localisation of the LUMO level on the acceptor moiety as the M_w of the polymer increases.[39] We speculate that the low M_w of **PTATffBT** results in the polymer displaying poor charge transport properties owing to a higher concentration of polymer chain ends and decreased packing density.

PPATBT-8 and **PPAT2BT-8** synthesised by Iraqi *et al* had HOMO/LUMO levels of -5.48/-3.14 eV and -5.35/-3.11 eV, respectively.[33] Clearly, the electronic properties of the resulting polymer are changed significantly when the substituents attached at the 9,10-positions of anthracene are modified. The TIPS group is fully conjugated to the anthracene π-system (resonance effect) and the *sp* hybridised acetylene carbons are more electron withdrawing than the sp^2 hybridised orbitals carbons to which they are attached (inductive effect). Thus, polymers that incorporate TIPS groups induce efficient intramolecular charge separation resulting in a notable decrease in the LUMO level.

Thermal Properties

The thermal properties of all conjugated polymers were investigated using thermograviemtric analysis (TGA). The resulting thermograms of the polymers are plotted in Figure 3. All polymers possess good thermal stability with degradation temperatures (5 % weight loss) in excess of 300°C; a desirable property for the fabrication of organic photovoltaic devices. **PTATffBT**, **PTATBT-8** and **PTAT2BT-8** display degradation temperatures of 352, 334 and 341°C, respectively. We speculate that the degradation temperatures of **PTATBT-8** and **PTAT2BT-8** are lower than that of **PTATffBT** as a result of fluorine substitution.[35,40,41] It Is speculated the octyloxy substituents attached to the 5,6-positions of benzothiadiazole in **PTATBT-8** and **PTAT2BT-8** are more thermally labile relative to fluorine.

Powder X-Ray Diffraction Studies

Powder X-ray diffraction (XRD) studies were conducted on the three polymers (Figure 4). The XRD patterns **PTATBT-8** and **PTAT2BT-8** display broad diffraction peaks at the angle of *ca.* 22° and is associated with π-π stacking. This x-ray diffraction pattern is consistent with many other amorphous donor-acceptor conjugated copolymers, for example PCDTBT.[42]

RSC Advances Accepted Manuscript

This journal is © The Royal Society of Chemistry 20xx

Please do not adjust margins
View Article Online
DOI: 10.1039/C5RA20927G

Journal Name

ARTICLE

Published on 18 November 2015. Downloaded by UNIVERSITY OF OTAGO on 20/11/2015 05:59:15.

Table 2. Performance of glass/ITO/PEDOT:PSS/polymer : $PC_{70}BM$/Ca/Al BHJ polymer solar cells under a simulated photovoltaic light with 1000 Wm^{-2} illumination (AM 1.5). PCE values given represent the highest and average values obtained.

Polymer	Polymer : $PC_{70}BM$[a] (w/w)	Solvent	J_{sc} (mA cm^{-2})	V_{oc} (V)	FF	PCE (%)	Thickness(nm)
PTATBT-8	1 :3	CF[b]	-6.66	0.88	37.5	2.20 (2.11 ± 0.10)	70
	1 :3	CB[c]	-6.88	0.90	37.8	2.36 (2.28 ± 0.07)	70
	1 :3	CB + DIO[d]	-4.26	0.86	49.4	1.80 (1.69 ± 0.10)	75
PTAT2BT-8	1 :3	CF[b]	-8.37	0.74	50.0	3.15 (2.99 ± 0.11)	75
	1 :3	CB[c]	-8.30	0.78	41.8	2.72(2.56±0.10)	85
	1 :3	CB + DIO[d]	-4.27	0.78	65.3	2.19 (2.08 ± 0.08)	85

[a]Polymer:$PC_{70}BM$ weight ratio. [b]CF = chloroform. [c]CB = chlorobenzene. [d]CB + DIO = chlorobenzene + diiodooctane (3 % additive).

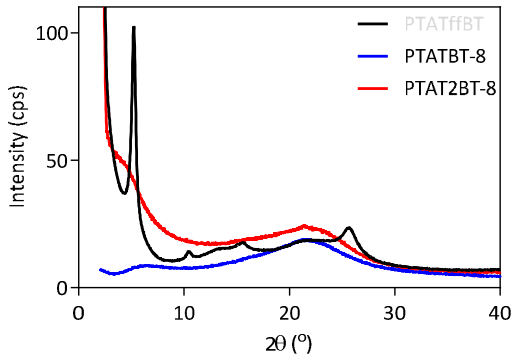

Figure 4. Powder XRD patterns of **PTATffBT**, **PTATBT-8** and **PTAT2BT-8**.

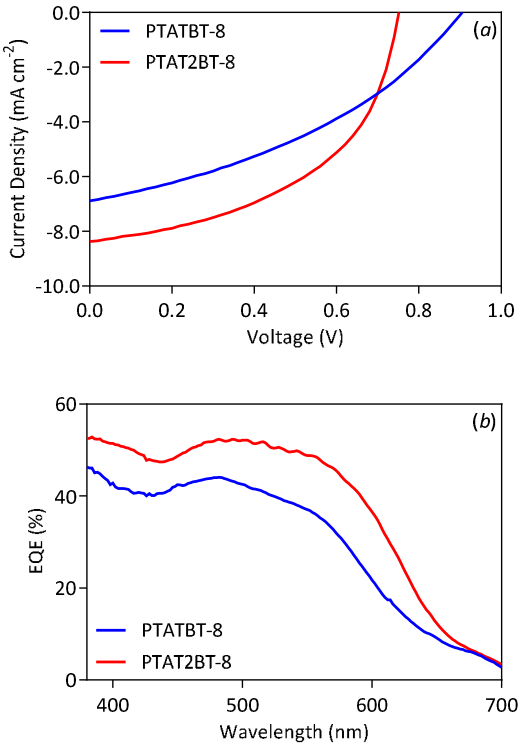

Figure 5.(*a*) *J-V* characteristic curves of photovoltaic devices fabricated from **PTATBT-8** and **PTAT2BT-8**; and (*b*) External quantum efficiency (EQE) spectra of corresponding devices measured using a monochromatic light source.

The XRD pattern of **PTATffBT** displays multiple diffraction peaks ranging from 5.27° to 25.7°. Previous literature has shown that the sharp intense peak at 5.27° corresponds to the distance between polymer main chains, where the solubilising alkyl chains organise in an interdigitated manner.[43,44] The peak at the wide angle of 25.7° corresponds to a π-π stacking distance of 3.7 Å. The smaller π-π stacking peak exhibited by **PTATffBT**, relative to **PTATBT-8** and **PTAT2BT-8**, can be attributed to the different substituents attached to the benzothiadiazole moiety with octyloxy substituents being larger and more sterically demanding than fluorine. The presence of sharp peaks in both the wide-angle and small-angle region suggests that **PTATffBT** adopts a more crystalline (possibly microcrystalline or semicrystalline) arrangement in solid state as a result of self-organisation of polymer chains forming more ordered domains in the solid state. This will reduce the solubility of **PTATffBT** in organic solvents, as well as limit its miscibility with the electron acceptor $PC_{70}BM$. Compared with that of **PTATffBT**, the miscibility of $PC_{70}BM$ with amorphous **PTATBT-8** and **PTAT2BT-8** is superior, and therefore enables moderate power conversion efficiencies.

RSC Advances Accepted Manuscript

Please do not adjust margins

View Article Online
DOI: 10.1039/C5RA20927G

Published on 18 November 2015. Downloaded by UNIVERSITY OF OTAGO on 20/11/2015 05:59:15.

Photovoltaic Properties

Photovoltaic measurements were made on a series of glass/ITO/PEDOT:PSS/polymer : $PC_{70}BM$/Ca/Al devices using blends of polymers : $PC_{70}BM$ in weight ratios from 1 : 1 to 1 : 4.

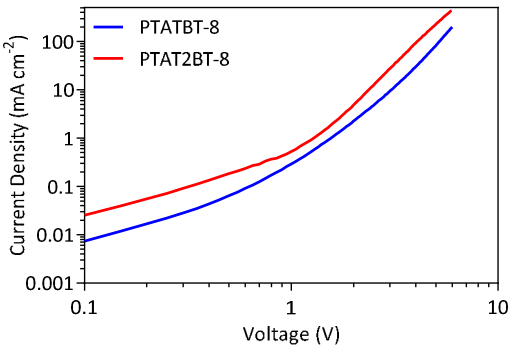

Figure 6. Dark *J-V* curves of hole only devices fabricated from **PTATBT-8** and **PTAT2BT-8**.

A detailed device-fabrication process is described in the Experimental section. As mentioned previously, the limited solubility of **PTATffBT** meant that photovoltaic devices could not be fabricated using this polymer. Photovoltaic measurements revealed that devices with the active layer cast from 1:3 polymer:$PC_{70}BM$ (w/w ratio) had optimum performance. The influence of casting solvent and additives were also investigated (see Table 2). A chlorobenzene casting solvent yielded the best results for **PTATBT-8** whilst chloroform was found to be the best solvent for **PTAT2BT-8**. The addition of 3.0% diiodooctane (DIO) as an additive did not improve the photovoltaic properties of the polymer but had a detrimental effect on the photovoltaic performance. The *J-V* characteristic curves for the best performing devices are shown in Figure 5*a*.

Both **PTATBT-8** and **PTAT2BT-8** exhibit modest performances with PCEs of 2.36 and 3.15 %, respectively. Optimised photovoltaic devices fabricated from **PTATBT-8** demonstrated an open-circuit voltage (V_{oc}) of 0.90 V, a short-circuit current (J_{sc}) of -6.88 mA cm^{-2} and a fill-factor (*FF*) of 37.8 %. In contrast, **PTAT2BT-8** displayed a V_{oc} of 0.74 V, a J_{sc} of -8.37 mA cm^{-2} and a *FF* of 50.0 %. The higher J_{sc} and *FF* of **PTAT2BT-8**, relative to **PTATBT-8**, presumably arise as a result of improved packing of polymer chains in polymer:$PC_{70}BM$ blends as a result of improving charge mobility and thus extraction of photo-generated charge carriers. It is well documented that the V_{oc} of photovoltaic devices is closely related to the energy difference between the HOMO of the donor and the LUMO level of the acceptor.[45] The lower HOMO level of **PTAT2BT-8**, relative to **PTATBT-8** is thus translated into a higher V_{oc} value. External quantum efficiencies (EQE) for corresponding devices were measured (Figure 5*b*). **PTAT2BT-8** demonstrated higher EQEs in excess of 45% between a wider range of wavelengths (380 – 576 nm) with a peak value of 52 % at 384 nm. In contrast, **PTATBT-8** demonstrated EQEs in excess of 45 % between a shorter range of wavelengths (380 – 388 nm) with a peak value of 46 % at 380 nm. The higher EQE corresponds to improved charge carrier separation and transportation properties, which is consistent with the higher J_{sc} values recorded for photovoltaic devices fabricated from **PTAT2BT-8**.

Hole-only devices were fabricated using the structure glass/ITO/PEDOT:PSS/polymer:$PC_{70}BM$/Au. The dark *J-V* curves of hole-only devices are presented in Figure 6. Following the space charge limited current (SCLC) theory, the hole mobilities of the two polymer:$PC_{70}BM$ films was calculated.[46] The hole mobility of **PTAT2BT-8**:$PC_{70}BM$ blends (9.7 x 10^{-5} cm^2 V^{-1} s^{-1}) is higher than **PTATBT-8**:$PC_{70}BM$ blends (1.6 x 10^{-5} cm^2 V^{-1} s^{-1}). **PTAT2BT-8** displays a higher hole mobility relative to **PTATBT-8** despite it possessing a lower molecular weight. We speculate this is a consequence of the incorporation of additional thiophene spacer units in **PTAT2BT-8**. These promote planarity of the polymer backbone which facilitates charge transportation. Taking both the EQE and hole mobility characterisation into consideration, the improved photovoltaic performance of **PTAT2BT-8**:$PC_{70}BM$ based devices can be attributed to improved charge carrier separation and subsequent charge extraction.

PPATBT-8 and **PPAT2BT-8** synthesised by Iraqi *et al* displayed PCEs of 3.92 and 4.17 %, respectively.[33] These are higher than the TIPS-functionalised polymers synthesised. This occurs as a result of higher J_{sc} and *FF* values for **PPATBT-8** and **PPAT2BT-8** to their comparable TIPS-functionalised analogues. Surprisingly, the smaller optical and electrochemical band-gaps of **PTATBT-8** and **PTAT2BT-8** did not translate into a larger J_{sc} values.

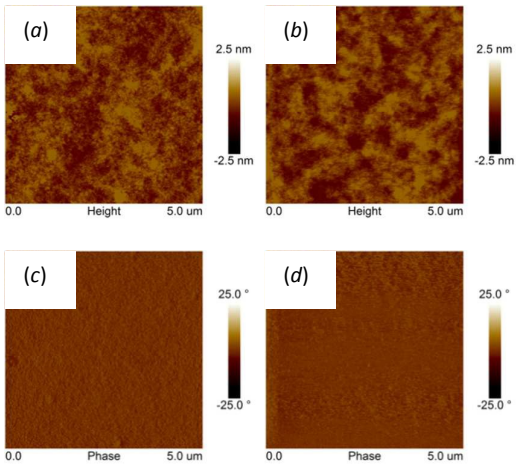

Figure 7. Tapping-mode atomic force microscopy topography (a and b) and phase images (c and d) of: **PTATBT-8** : $PC_{70}BM$ (1:3 w/w) (a and c); and **PTAT2BT-8** : $PC_{70}BM$ (1:3 w/w) (b and d).

RSC Advances Accepted Manuscript

This journal is © The Royal Society of Chemistry 20xx

Please do not adjust margins
View Article Online
DOI: 10.1039/C5RA20927G

Published on 18 November 2015. Downloaded by UNIVERSITY OF OTAGO on 20/11/2015 05:59:15.

Atomic Force Microscopy (AFM) Images

Atomic force microscopy (AFM) in tapping mode was used to image the surface morphologies of **PTATBT-8**:$PC_{70}BM$ (1:3) and **PTAT2BT-8**:$PC_{70}BM$ (1:3) blend films spin-coated from chlorobenzene and chloroform solutions respectively, as shown in Figure 7. It should be noted that there is no significant difference in the surface morphologies of the **PTATBT-8** and **PTAT2BT-8** based blends. Both exhibit smooth, amorphous looking surfaces with no indication of unfavourable large-scale phase separation. Such morphologies should result in efficient excitation and photocharge generation. As AFM reveal no significant difference in the surface morphologies of the two types of blend film we tentatively speculate that the improved J_{sc} associated with devices fabricated from **PTAT2BT-8** are a result of difference in improved charge carrier separation and transportation properties, as evidenced by the EQE spectra. This is also reflected by the improved *FF* associated with devices fabricated from **PTAT2BT-8**; a property that results from improved charge-carrier mobility.

Conclusions

Three triisopropylsilylacetylene-functionalised anthracene (TIPSAnt) based polymers were synthesised by copolymerising TIPSAnt with either dithienyl-5,6-difluoro-benzo[*c*]-[1,2,5]thiadiazole, dithienyl-benzo[*c*]-[1,2,5]thiadiazole or dibithiophenyl-benzo[*c*]-[1,2,5]thiadiazole to yield **PTATffBT**, **PTATBT-8** and **PTAT2BT-8**, respectively. Whilst chemical characterisation of **PTATffBT** was possible, the limited solubility of the conjugated polymer in common organic solvents at elevated temperatures meant that fabrication of BHJ photovoltaic devices *via* solution processing was not possible. Both **PTATBT-8** and **PTAT2BT-8** displayed excellent solubility in common organic solvents; a consequence of the incorporation of octyloxy-chains onto the 5,6-positions of the benzothiadiazole acceptor-moiety. UV-visible spectroscopy revealed that **PTAT2BT-8** had the lowest optical band gap of all polymers synthesised with a value of 1.81 eV. We find that **PTATffBT** had the deepest HOMO level (-5.48 eV); a consequence of utilising a fluorinated-benzothiadiazole acceptor monomer. **PTATBT-8** and **PTAT2BT-8**had HOMO levels of -5.46 and -5.31 eV. The addition of an additional thiophene spacer unit in **PTAT2BT-8** increases intramolecular charge transfer along the polymer backbone resulting in a shallower HOMO level relative to **PTATBT-8**. BHJ photovoltaic devices fabricated from **PTATBT-8**:$PC_{70}BM$ and **PTAT2BT-8**:$PC_{70}BM$ had efficiencies of 2.36 and 3.15 %, respectively. The improved PCE values of **PTAT2BT-8** occur primarily as a result of increased J_{sc} and *FF*. Taking both the EQE and hole mobility characterisation into consideration the improved photovoltaic performance of **PTAT2BT-8**:$PC_{70}BM$ based devices can be attribute to improved charge carrier separation and charge transportation.

Experimental Section

Materials

4.7-Bis(5-bromothiophen-2-yl)-5,6-difluorobenzo[c][1,2,5]thiadiazole(**M2**),[47,48] 4,7-bis-(5-bromo-thiophen-2-yl)-5,6-bis-octyloxy-benzo[*c*][1,2,5]thiadiazole (**M3**)[49] and 4,7-bis-(5'-bromo-[2,2']bithiophenyl-5-yl)-5,6-bis-octyloxy-benzo-[1,2,5]thiadiazole (**M4**)[50] were prepared according to previous established literature procedures. $PC_{70}BM$ (95 %) was purchased from Ossila Ltd. All chemicals and solvents, with the exception of those stated below, were of reagent grade quality, purchased commercially and used without further purification unless otherwise stated. Toluene was dried and distilled over sodium under an inert argon atmosphere. Acetonitrile (high performance liquid chromatography (HPLC) grade) was dried and distilled over phosphorous pentoxide under an inert argon atmosphere, then stored over molecular sieves, 3 A.

Measurements

^{1}H and ^{13}C nuclear magnetic resonance (NMR) spectra were recorded on either Bruker AV 250 (250 MHz), Bruker AV 400 (400 MHz) or Bruker Avance III HD 500 (500 MHz) spectrometers at room temperature, using chloroform-d ($CDCl_3$) or at 100°C using 1,2-dideutrotetrachloroethane as the solvent. NMR spectra were recorded in parts per million (ppm) relative to tetramethysilane (δ_H0.00). Coupling constants are given in hertz (Hz). Carbon, nitrogen and sulphur elemental analysis was performed on a Perkin Elmer 2400 series 11 CHNS/O analyser. Analysis of halides was undertaken using the Schöniger flask combustion method. GPC analysis was conducted on polymer solutions in 1,2,4-trichlorobenzene at 140°C. Polymer samples were spiked with toluene as a reference. GPC curves were obtained using a Viscotek GPC_{max} VE 2001 GPC solvent/ sample module and a Waters 410 Differential Refractometer, which was calibrated using a series of narrow polystyrene standards (Polymer Laboratories). TGA traces were obtained using a Perkin Elmer TGA-1 Thermogravimetric Analyser at a scan rate of 10 °C min^{-1} under an inert nitrogen atmosphere. Powder XRD samples were recorded on a Bruker D8 Avance diffractometer with a CuKα radiation source (1.5418 Å, rated as 1.6 kW). The scanning angle was conducted over the range 2-40°. UV-visible absorption spectra were recorded at ambient temperature using a Hitachi U-2010 Double Beam UV/Visible Spectrophotometer. Polymer solutions were made using chloroform (spectrophotometric grade) and measured using quartz cuvettes (path length = 1 x10^{-2} m). Thin films used for absorption spectra were prepared by drop casting solutions onto quartz plates using 1 mg cm^{-3}polymer solutions that were prepared using chloroform (HPLC grade). Cyclic voltammograms were recorded using a Princeton Applied Research Model 263A Potentiostat/Galvanostat. A three electrode system was employed comprising a Pt disc (area = 3.14 x 10^{-2} cm^2), platinum wire and Ag/Ag^+ as the working electrode, counter electrode and reference electrode, respectively, in a tetrabutylammonium perchlorate acetonitrile

RSC Advances Accepted Manuscript

Please do not adjust margins

View Article Online
DOI: 10.1039/C5RA20927G

Published on 18 November 2015. Downloaded by UNIVERSITY OF OTAGO on 20/11/2015 05:59:15.

solution (0.1 mol dm^{-3}). Measurements were conducted on polymer films that were prepared by drop casting 1.0 mm^3 of polymer solution (1 mg cm^{-2} in chloroform (HPLC grade)). In accordance with IUPAC's recommendations, ferrocene was employed as a reference redox system.[51]

Fabrication and Testing of BHJ polymer solar cells

The polymers and $PC_{70}BM$ were dissolved separately in either CF, CB or CB with 3 % DIO, and were then put on a hot plate held at 70°C overnight with stirring to allow dissolution. The solutions were then mixed at different polymer:fullerene blend ratios before spin casting. Photovoltaic devices were fabricated onto pre-patterned ITO glass substrates (20 Ohms per square) that were supplied by Ossila Limited. The ITO/glass substrates were first cleaned by sonication in dilute NaOH followed by IPA. A 30 nm thick PEDOT:PSS layer was spin-coated onto the ITO/glass substrates. These were then transferred to a hot-plate held at 120°C for 10 minutes before being transferred to a nitrogen glove-box. All active layers were spin cast onto the glass/ITO/PEDOT:PSS substrate. The devices were then transferred into a thermal evaporator for deposition of a cathode (5 nm of calcium followed by a 100 nm of aluminium evaporated at a base pressure of ~ 10^{-7} mbar). The cathode was deposited through a shadow-mask producing a series of independent pixels. Devices were encapsulated using a glass slide and epoxy glue before testing. PCEs were determined using a Newport 92251A-1000 AM 1.5 solar simulator. An NREL calibrated silicon cell was used to calibrate the power output to 100 mW cm^{-2} at 25°C. An aperture mask having an area of 2.06 mm^2 was placed over devices to define the test area. At least two devices were prepared for each sample to give 12 pixels. Each reporting an independent *J-V* curve. EQE values were determined over the wavelength range of interest by comparing the photocurrent of the OPV cell to a reference silicon photodiode having a known spectral response.

2,6-Bis-(4,4,5,5-tetramethyl-1,3,2-dioxaborolan-2-yl)-9,10-bis(triisopropylsilylacetylene) anthracene (M1)

A single neck round bottom containing 2,6-dibromo-9,10-bis(triisopropylsilylacetylene)anthracene (3.00 g, 4.3 mmol), bis(pinacolato)diboron (3.83 g, 15.01 mmol), potassium acetate (2.52 g, 24.97 mmol) and $Pd(dppf)Cl_2$ (0.2 g, 0.25 mmol) was placed under an argon atmosphere using standard schlenk line techniques. To this mixture, DMF (50 cm^3) was added, degassed and heated at 90°C for 48 hours. The reaction mixture was cooled to room temperature and poured into water (50 cm^3) and extracted with diethyl ether (3 x 100 cm^3). The organic phases were combined, washed with H_20 (2 x 100cm^3) and dried ($MgSO_4$). The crude product was purified by dissolving in the minimum amount of hot ether and precipitated in methanol which had been run through a basic column (1.41 g, 1.8 mmol, 41 %). ^{1}H NMR (250 MHz, $CDCl_3$): (δ_H/ppm) 9.30 (s, 2H) 8.62 (d, *J* = 8.48 Hz, 2H), 7.94 (dd, *J* = 0.98 Hz and *J* = 8.48 Hz, 2H), 1.41 (s, 24H), 1.32 (m, 42H). ^{13}C NMR (250 MHz, $CDCl_3$) ∂ (ppm): 136.42, 133.44, 132.37, 130.61, 126.91, 105.22, 103.33, 83.93, 25.00, 18.94, 11.58. $[M]^+$ calculated for$C_{48}H_{72}B_2O_4Si_2$, 790.515529; found, 790.513046. Elemental Analysis (%) calculated for $C_{48}H_{72}B_2O_4Si_2$: C, 72.90; H, 9.18. Found: C, 73.22; H, 7.72.

Poly[9,10-bis(triisopropylsilylacetylene)-anthracene-2,6-diyl-alt-(4,7-dithiophen-2-yl)-5,6-difluorobenzo[c][1,2,5]thiadiazole-5-5-diyl] (PTATffBT):4.7-Bis(5-bromothiophen-2-yl)-5,6-difluorobenzo[c][1,2,5]thiadiazole (0.181 g, 0.367 mmol) and 2,6-bis-(4,4,5,5-tetramethyl-1,3,2-dioxaborolan-2-yl)-9,10-bis(triisopropylsilylacetylene) anthracene (0.290 g, 0.367 mmol) were added to a flask and placed under an inert argon atmosphere using standard schlenk line techniques. Dry toluene (9 cm^3) and tetraethyl ammonium hydroxide (20 % wt, 2 cm^3, degassed) were added and the reaction was degassed again. $Pd(OAc)_2$ (6.5 mg, 28.9 µmol) and tri(o-tolyl)phosphine (17.3 mg, 56.8 µmol) was added and the reaction mixture was degassed again. The mixture was heated to 90°C for 30 minutes. Upon completion, the mixture was cooled to room temperature and bromobenzene (0.1 cm^3, 0.94 mmol) was added. The mixture was degassed and heated at 90°C for 1 hour. Upon completion, the reaction mixture was cooled to room temperature and phenyl boronic acid (150 mg, 1.23 mmol) was added. The mixture was degassed and heated at 90°C for a further hour. The mixture was cooled to room temperature and precipitated into methanol (500 cm^3, degassed) and stirred overnight. The resulting mixture was filtered through a membrane filter and the polymer was obtained as a deep purple powder. The polymer was cleaned using Soxhlet extraction with solvents in the following order: methanol, acetone, hexane and toluene. The toluene fraction was concentrated (~ 50 cm^3) and then poured into degassed methanol (500 cm^3). The resulting mixture was stirred overnight and the solid was collected by filtration (92.4 mg, 29 %). GPC analysis: Mn = 2,100 Da, Mw = 2,500 Da, PDI = 1.19. ^{1}H-NMR (500 MHz, $C_2D_2Cl_4$, 100°C) (δ_H/ppm) 8.96 (m, 1H), 8.77-8.52 (m, 2H), 8.38-8.20 (m, 2H), 7.97 (m, 1H), 7.67 (m, 2H), 7.49-7.27 (m, 2H).^{19}F-NMR (500 MHz, $C_2D_2Cl_4$, 100°C) (δ_F/ppm) -127.22, -127.70.Anal.Calcd.for $C_{50}H_{52}F_2N_2S_3Si_2$: C, 68.92; H 6.02; N, 3.22; S, 11.04. Found: C, 67.85; H, 5.93; N, 2.78; S, 9.68.

Poly[9,10-bis(triisopropylsilylacetylene)-anthracene-2,6-diyl-alt-(5,6-bis(octyloxy)-4,7-di(thiophene-2-yl)benzo[c]thiadiazole-5,5-diyl] (PTATBT-8):PTATBT-8 was synthesized according to the polymerisation method outlined for **PTATffBT**: 4,7-bis(5-bromo-2-thienyl)-5,6-bis(octyloxy)-2,1,3-benzothiadiazole (0.262 g, 0.367 mmol) and 2,6-bis-(4,4,5,5-tetramethyl-1,3,2-dioxaborolan-2-yl)-9,10-bis(triisopropylsilylacetylene) anthracene (0.290 g, 0.367 mmol) were added to a flask and placed under an inert argon atmosphere using standard schlenk line techniques. Dry toluene (10 cm^3) and tetraethyl ammonium hydroxide (20 % wt, 2.1 cm^3, degassed) were added and the reaction was degassed again. $Pd(OAc)_2$ (6.0 mg, 26.7 µmol) and tri(o-tolyl)phosphine (16.3 mg, 53.6 µmol) was added and the

RSC Advances Accepted Manuscript

This journal is © The Royal Society of Chemistry 20xx

Please do not adjust margins
View Article Online
DOI: 10.1039/C5RA20927G

Published on 18 November 2015. Downloaded by UNIVERSITY OF OTAGO on 20/11/2015 05:59:15.

reaction mixture was degassed again. The mixture was heated to 90°C. The polymerisation was deemed complete after 3 hours. The polymer was obtained as a purple solid (230 mg, 57 %). GPC analysis: M_n = 13,600 Da, M_w = 38,700 Da, PDI = 2.84. ^{1}H-NMR (500 MHz, $C_2D_2Cl_4$, 100°C) (δ_H/ppm) 8.89 (br, 1H), 8.82-8.32 (m, 4H), 7.99 (br, 1H), 7.67 (br, 2H), 7.49-7.22 (m, 2H), 4.21 (br, 4H), 1.94 (br, 4H), 1.55-1.01 (m, 62H), 0.80 (br, 6H).Anal.Calcd.for $C_{66}H_{86}N_2O_2S_3Si_2$: C, 72.61; H 7.94; N, 2.57; S, 8.81. Found: C, 70.16; H, 6.55; N, 3.35; S, 10.35.

Poly(9,10-bis(triisopropylsilylacetylene)-anthracene-2,6-diyl-alt-(5,6-bis(octyloxy)-4,7-di(2,2'-bithiophen-5-yl)benzo[c][1,2,5]thiadiazole)-5,5-diyl] (PTAT2BT-8):PTAT2BT-8was synthesized according to the polymerisation method outlined for **PTATffBT**: 4,7-bis(5'-bromo-2,2'-bithien-5-yl)-5,6-bis(octyloxy)-2,1,3-benzothiadiazole (0.323 g, 0.367 mmol) and 2,6-bis-(4,4,5,5-tetramethyl-1,3,2-dioxaborolan-2-yl)-9,10-bis(triisopropylsilylacetylene) anthracene (0.290 g, 0.367 mmol) were added to a flask and placed under an inert argon atmosphere using standard schlenk line techniques. Dry toluene (10 cm^3) and tetraethyl ammonium hydroxide (20 % wt, 2.1 cm^3, degassed) were added and the reaction was degassed again. $Pd(OAc)_2$ (6.1 mg, 27.2 µmol) and tri(o-tolyl)phosphine (16.1 mg, 53.0 µmol) was added and the reaction mixture was degassed again. The mixture was heated to 90°C. The polymerisation was deemed complete after 1 hour. The polymer was obtained as a deep purple solid. (76.7 mg, 17 %). GPC analysis: M_n = 6,600 Da, M_w = 13,200 Da, PDI = 2.00. ^{1}H-NMR (500 MHz, $C_2D_2Cl_4$, 100°C) (δ_H/ppm) 8.87 (s, 1H), 8.62 (d, 2H, *J* = 8.50 Hz), 8.44 (m, 2H), 7.88 (d, 2H, *J* = 8.50 Hz), 7.67-6.95 (m, 9H), 4.20 (br, 4H), 1.97 (br, 4H), 1.56-1.09 (m, 62H), 0.86 (br, 6H). Anal.Calcd.for $C_{74}H_{90}N_2O_2S_5Si_2$: C, 70.67; H 7.22; N, 2.23; S, 12.76. Found: C, 71.01; H, 7.01; N, 2.92; S, 14.98.

Acknowledgements

We would like to thank EPSRC for financial support of this work *via* research grants EP/J017361/1 and EP/I028641/1. YZ thanks the University of Sheffield for the award of a scholarship. TW acknowledges financial support from the Recruitment Program of Global Experts and the Natural Science Foundation of China (Grant No. 21504065).

References

1. G. Dennler, M. C. Scharber and C. J. Brabec, *Adv. Mater.*, 2009, **21**, 1323–1338.

2. J. Y. Kim, K. Lee, N. E. Coates, D. Moses, T. Nguyen, M. Dante and A. J. Heeger, *Science (80-.).*, 2007, **317**, 222–226.

3. Y. G, J. Gao, J. C. Hummelen, F. Wudl and A. J. Heeger, *Science (80-.).*, 1995, **80**, 1789–1791.

4. Y. Liu, J. Zhao, Z. Li, C. Mu, W. Ma, H. Hu, K. Jiang, H. Lin, H. Ade and H. Yan, *Nat. Commun.*, 2014, **5**, 1–8.

5. M. C. Scharber and N. S. Sariciftci, *Prog. Polym. Sci.*, 2013, **38**, 1929–1940.

6. J.-D. Chen, C. Cui, Y.-Q. Li, L. Zhou, Q.-D. Ou, C. Li, Y. Li and J.-X. Tang, *Adv. Mater.*, 2015, **27**, 1035–1041.

7. S. Günes, H. Neugebauer and N. S. Sariciftci, *Chem. Rev.*, 2007, **107**, 1324–1338.

8. M. M. Wienk, J. M. Kroon, W. J. H. Verhees, J. Knol, J. C. Hummelen, P. A. Van Hal and R. A. J. Janssen, *Angew. Chemie - Int. Ed.*, 2003, **42**, 3371–3375.

9. C. J. Brabec, G. Zerza, G. Cerullo, S. De Silvestri, S. Luzzati, J. C. Hummelen and S. Sariciftci, *Chem. Phys. Lett.*, 2001, **340**, 232–236.

10. J. W. Arbogast and C. S. Foote, *J. Am. Chem. Soc.*, 1991, **113**, 8886–8889.

11. L. Chen, P. Shen, Z. Zhang and Y. Li, *J. Mater. Chem. A*, 2015, **3**, 12005–12015.

12. D. Mühlbacher, M. Scharber, M. Morana, Z. Zhu, D. Waller, R. Gaudiana and C. Brabec, *Adv. Mater.*, 2006, **18**, 2884–2889.

13. R. R. Søndergaard, M. Hösel and F. C. Krebs, *J. Polym. Sci. Part B Polym. Phys.*, 2013, **51**, 16–34.

14. R. Søndergaard, M. Hösel, D. Angmo, T. T. Larsen-Olsen and F. C. Krebs, *Mater. Today*, 2012, **15**, 36.

15. H. Kallmann and M. Pope, *J. Chem. Phys.*, 1959, **30**, 585–586.

16. Y. Li, T.-H. Kim, Q. Zhao, E.-K. Kim, S.-H. Han, Y.-H. Kim, J. I. N. Jang and S.-K. Kwon, *J. Polym. Sci. Part A Polym. Chem.*, 2008, **46**, 5115–5122.

17. C. Liu, W. Cai, X. Guan, C. Duan, Q. Xue, L. Ying, F. Huang and Y. Cao, *Polym. Chem.*, 2013, **4**, 3949–3958.

18. J. W. Jung and W. H. Jo, *Polym. Chem.*, 2015, **6**, 4013–4019.

19. C. Liu, W. Xu, X. Guan, H. Yip, X. Gong, F. Huang and Y. Cao, *Macromolecules*, 2014, **47**, 8585–8593.

20. D. A. M. Egbe, S. Türk, S. Rathgeber, F. Kühnlenz, R. Jadhav, A. Wild, E. Birckner, G. Adam, A. Pivrikas, V. Cimrova, G. Knör, N. S. Sariciftci and H. Hoppe, *Macromolecules*, 2010, **43**, 1261–1269.

RSC Advances Accepted Manuscript

Please do not adjust margins

View Article Online
DOI: 10.1039/C5RA20927G

21. D. A. M. Egbe, G. Adam, A. Pivrikas, A. M. Ramil, E. Birckner, V. Cimrova, H. Hoppe and N. S. Sariciftci, *J. Mater. Chem.*, 2010, **20**, 9726–9734.

22. J. I. N. U. K. Ju, D. A. E. S. Chung, S. O. N. G. Kim, S. O. U. K. Jung, C. E. O. N. Park, Y. Kim and S. Kwon, *J. Polym. Sci. Part A Polym. Chem.*, 2009, **47**, 1609–1616.

23. H. Meng, F. Sun, M. B. Goldfinger, G. D. Jaycox, Z. Li, W. J. Marshall and G. S. Blackman, *J. Am. Chem. Soc.*, 2005, **127**, 2406–2407.

24. J. Y. Back, T. K. An, Y. R. Cheon, H. Cha, J. Jang, Y. Kim, Y. Baek, D. S. Chun, S.-K. Kwon, C. E. Park and Y.-H. Kim, *ACS Appl. Mater. Interfaces*, 2015, **7**, 351–3528.

25. H.-J. Yun, D. S. Chung, I. Kang, J. W. Park, Y.-H. Kim and S.-K. Kwon, *J. Mater. Chem.*, 2012, **22**, 24924–24929.

26. S. Tao, Y. Zhou, C.-S. Lee, S.-T. Lee, D. Huang and X. Zhang, *J. Phys. Chem. C*, 2008, **112**, 14603–14606.

27. J. Huang, J. Su and H. Tian, *J. Mater. Chem.*, 2012, **22**, 10977–10989.

28. H. Kim, H. Lee, D. Seo, Y. Jeong, K. Cho, J. Lee and Y. Lee, *Chem. Mater.*, 2015, **27**, 3102–3107.

29. S. Liu, X. Bao, W. Li, K. Wu, G. Xie, R. Yang and C. Yang, *Macromolecules*, 2015, **48**, 2948–2957.

30. L. Huo and J. Hou, *Polym. Chem.*, 2011, **2**, 2453–2461.

31. W. Chen, Z. Du, L. Han, M. Xiao, W. Shen, T. Wang, Y. Zhou and R. Yang, *J. Mater. Chem. A*, 2015, **3**, 3130–3135.

32. J.-H. Park, D. S. Chung, D. H. Lee, H. Kong, I. H. Jung, M.-J. Park, N. S. Cho, C. E. Park and H.-K. Shim, *Chem. Commun.*, 2010, **46**, 1863–1865.

33. M. S. Almeataq, H. Yi, S. Al-Faifi, A. A. B. Alghamdi, A. Iraqi, N. W. Scarratt, T. Wang and D. G. Lidzey, *Chem. Commun.*, 2013, **49**, 2252–2254.

34. J. Park, D. S. Chung, J. Park, T. Ahn, H. Kong, Y. K. Jung, J. Lee, M. H. Yi, C. E. Park, S.-K. Kwon and H. Shim, *Org. Lett.*, 2007, **9**, 2573–2576.

35. L. Cartwright, A. Iraqi, Y. Zhang, T. Wang and D. G. Lidzey, *RSC Adv.*, 2015, **5**, 46386–46394.

36. T. Umeyama, Y. Watanabe, E. Douvogianni and H. Imahori, *J. Phys. Chem. C*, 2013, **117**, 21148–21157.

37. Y. Zhang, S.-C. Chien, K.-S. Chen, H.-L. Yip, Y. Sun, J. A. Davies, F.-C. Chen and A. K. Y. Jen, *Chem. Commun.*, 2011, **47**, 11026–11028.

38. D. Dang, W. Chen, R. Yang, W. Zhu, W. Mammo and E. Wang, *Chem. Commun.*, 2013, **49**, 9335–9337.

39. B. Kim, X. Ma, C. Chen, Y. Ie, E. W. Coir, H. Hashemi, Y. Aso, P. F. Green, J. Kieffer and J. Kim, *Adv. Funct. Mater.*, 2013, **23**, 439–445.

40. Z. Li, J. Lu, S.-C. Tse, J. Zhou, X. Du, Y. Tao and J. Ding, *J. Mater. Chem.*, 2011, **21**, 3226–3233.

41. A. Iyer, J. Bjorgaard, T. Anderson and M. E. Köse, *Macromolecules*, 2012, **45**, 6380–6389.

42. T. Wang, A. J. Pearson, A. D. F. Dunbar, P. A. Staniec, D. C. Watters, H. Yi, A. J. Ryan, R. A. L. Jones, A. Iraqi and D. G. Lidzey, *Adv. Funct. Mater.*, 2012, **22**, 1399–1408.

43. S. H. Chen, A. C. Su and S. A. Chen, *J. Phys. Chem. B*, 2005, **109**, 10067–10072.

44. M. Grell, D. D. C. Bradley, G. Ungar, J. Hill and K. S. Whitehead, *Macromolecules*, 1999, **32**, 5810–5817.

45. M. C. Scharber, D. Mühlbacher, M. Koppe, P. Denk, C. Waldauf, A. J. Heeger and C. J. Brabec, *Adv. Mater.*, 2006, **18**, 789–794.

46. Y. Liang, Z. Xu, J. Xia, S. Tsai, Y. Wu, G. Li, C. Ray and L. Yu, *Adv. Energy Mater.*, 2010, **22**, 135–138.

47. N. Cho, K. Song, J. K. Lee and J. Ko, *Chem. - A Eur. J.*, 2012, **18**, 11433–11439.

48. H. Zhou, L. Yang, A. C. Stuart, S. C. Price, S. Liu and W. You, *Angew. Chemie - Int. Ed.*, 2011, **50**, 2995–2998.

49. R. Qin, W. Li, C. Li, C. Du, C. Veit, H.-F. Schleiermacher, M. Andersson, Z. Bo, Z. Liu, O. Inganäs, U. Wuerfel and F. Zhang, *J. Am. Chem. Soc.*, 2009, **131**, 14612–14613.

50. H. Yi, S. Al-Faifi, A. Iraqi, D. C. Watters, J. Kingsley and D. G. Lidzey, *J. Mater. Chem.*, 2011, **21**, 13649–13656.

51. G. Gritzner, *Pure Appl. Chem.*, 1990, **62**, 1839–1858.

Published on 18 November 2015. Downloaded by UNIVERSITY OF OTAGO on 20/11/2015 05:59:15.

RSC Advances Accepted Manuscript

This journal is © The Royal Society of Chemistry 20xx

View Article Online
DOI: 10.1039/C5RA20927G

Published on 18 November 2015. Downloaded by UNIVERSITY OF OTAGO on 20/11/2015 05:59:15.

Graphical contents entry for article:

Triisopropylsilylacetylene-Functionalised Anthracene-*alt*-Benzothiadiazole Copolymers for Application in Bulk Heterojunction Solar Cells

Luke Cartwright,[a] Lois. J. Taylor, [a] Hunan Yi, [a] Ahmed Iraqi,*[a] Yiwei Zhang,[b] Nicholas. W. Scarratt,[b] Tao Wang,[c] David. G. Lidzey*[b]

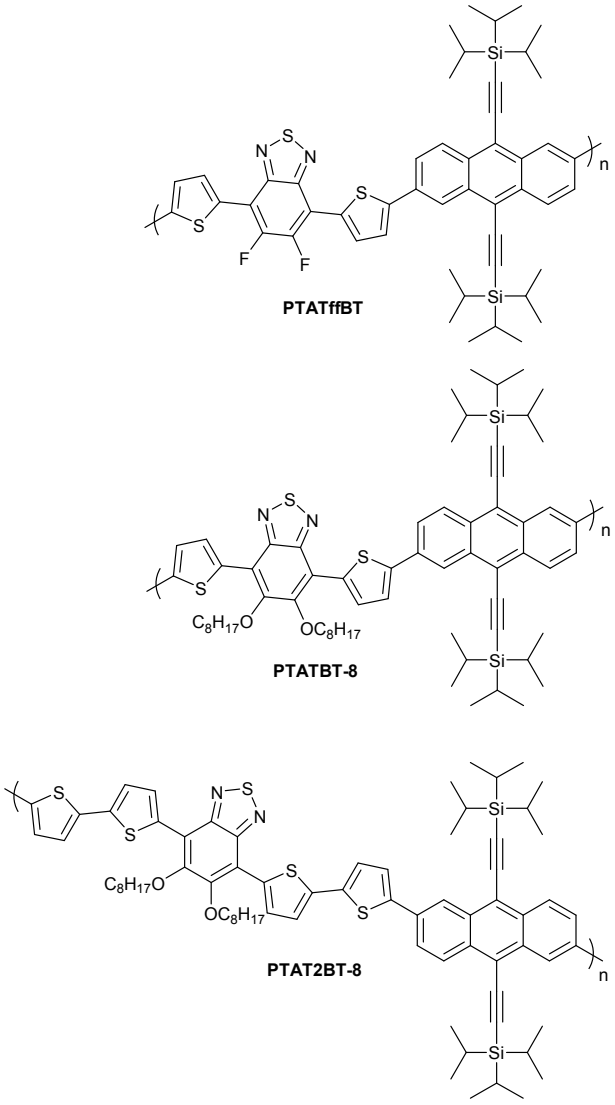

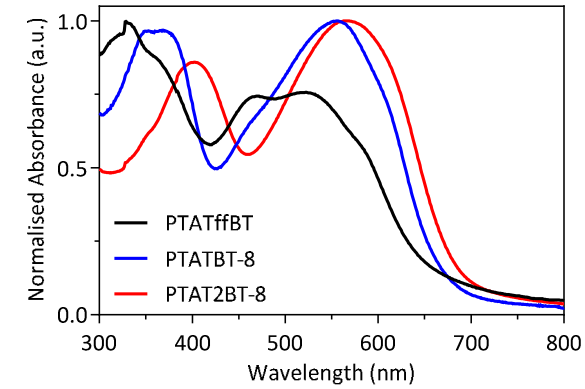

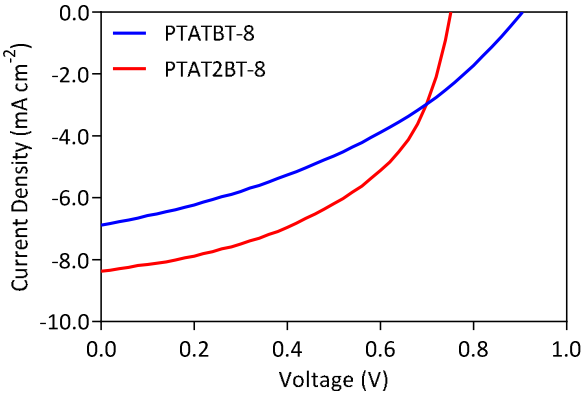

Three triisopropylsilylacetylene-functionalised anthracene (TIPSAnt) based polymers were synthesised by copolymerising TIPSAnt with either dithienyl-5,6-difluoro-benzo[*c*]-[1,2,5]thiadiazole, dithienyl-benzo[*c*]-[1,2,5]thiadiazole or dibithiophenyl-benzo[*c*]-[1,2,5]thiadiazole to yield **PTATffBT**, **PTATBT-8** and **PTAT2BT-8**, respectively. The optical, electrochemical, thermal, structural and photovoltaic properties in bulk heterojunction solar cells are investigated.

RSC Advances Accepted Manuscript